Photo-thermal Modeling of Plasmonic Heating of Concentric Nanoparticles

Meng Hu, Changhong Liu, and Ben Q. Li, *ASME Fellow*

Abstract— A modeling study on the energy absorption and heat transfer of concentric nanoparticles under localized surface plasma resonance (SPR) conditions is presented. A generalized theoretical formulation for multi-scattering of electromagnetic waves by multilayered nanoparticle is employed to determine the heat source first, and then starting with the Eigen functions, direct and inverse integral transform, needed for a non-homogeneous heat conduction problem defined over a multiple domain with an infinite boundary, is constructed.

***Index Terms*—**Surface plasmon resonance, photo-thermal, nanoparticle, heat conduction

I. Introduction

Gold structured nanoparticles have found a wide range of applications in photo-thermal therapy of cancer patients and optical bio-imaging [1-3]. A salient feature of this class of nanoparticles is that the localized surface plasma resonance, contributed by the collective oscillation of the conduction band electrons in a gold layer, can be tuned to a light source from visible light to near infrared region (NIR) by varying the structural parameters of the nanoparticle. One of the applications that has received considerable attention in recent years is to use gold nanoshells as a highly selective heat absorber for a near-infrared (NIR) laser to thermally-destroy cancerous tumors or deliver thermal-kill of bacteria or virus [4, 5]. Much of the research work in this area has been experimental, with intention to demonstrate the feasibility of the potential clinic application. Theoretical analysis has been mainly devoted to the photon-electron interactions using the Mie solution [6]. Little work appears to have been published on the integrated photo-thermal analysis of such systems.

This paper presents a combined photo-thermal analysis of concentric spherical gold nanoparticles excited by a plane wave within an NIR frequency. The Maxwell equations and heat conduction in multiple domains are solved analytically using the multipole expansion method and an integral transformation method. The methodology presented in the paper should work well for other heating problems that result from electric or magnetic origin.

Meng Hu is a master student of Department of Electrical Engineering ,Shanghai Jiao Tong University, Shanghai 200240 China. (e-mail: heishansiren@sjtu.edu.cn).

Changhong Liu is with Department of Electrical Engineering, Shanghai Jiao Tong University, Shanghai 200240, and Xi'an Jiaotong University, Shaanxi, China. (e-mail: liuch@ sjtu.edu.cn).

Ben Q. Li is with Department of Mechanical Engineering, University of Michigan, Dearborn, MI 48128 USA. (Corresponding author, Tel& Fax: 1-313-593-5465, e-mail: benqli@ umich.edu)

II. Mathematical Model

A. Laser-induced Joule heat

The computational model used in this study has been presented in detail elsewhere [7] and thus only an outline is given here. The model is developed to describe the multi-scattering of electromagnetic waves by an individual or an ensemble of concentric spherical particles of different sizes and of different shell thicknesses positioned at different locations. It solves the vector form of the Maxwell equations,

$$\nabla^2\mathbf{E}+k^2\mathbf{E}=0,\qquad \nabla\cdot\mathbf{E}=0,\qquad \mathbf{H}=-(i/\mu_0\omega)\nabla\times\mathbf{E} \quad (1)$$

where $\mathbf{E}$ is the electric field, $k^2=\varepsilon\mu m^2c$ with c being the speed of light, m the refractive index, ε the electric permittivity, ω the angular frequency, and μ the magnetic permeability.

The computational procedure starts with a recursive algorithm for the Mie solution for an isolated multilayered nanoshell. The nanoshell is essentially a spherical particle of L concentric layers, with each layer characterized by a size parameter $x_l = 2\pi\tilde{N}_l r_l/\lambda$ and a relative refractive index $m_l = \tilde{N}_l/\tilde{N}$, where λ is wavelength, r_l and $\tilde{N}_l$ are radius and refractive index of the lth layer (l = 1, 2, …, L), and $\tilde{N}$ is refractive index of the host media. By means of spherical eigenvectors, the electromagnetic field inside the lth layer is expanded as

$$\mathbf{E}_l=\sum_{n=1}^{\infty}E_n\left[c_n^l\mathbf{M}_{o1n}^{(1)}-id_n^l\mathbf{N}_{e1n}^{(1)}+ia_n^l\mathbf{N}_{e1n}^{(3)}-b_n^l\mathbf{M}_{o1n}^{(3)}\right] \quad (2)$$

where c_n and d_n are the coefficients of the wave functions for the internal field and are calculated recursively [16] and for an plane incident wave, $E_n=i^nE_0(2n+1)/n(n+1)$. For an aggregate of multilayered nanoshells, the scattered electromagnetic field for the ith nanoshell in the aggregate takes the following form,

$$\mathbf{E}_s(j)=\sum_{n=1}^{\infty}\sum_{m=-n}^{n}(a_{mn}^j\mathbf{m}_{mn}^{(3)}(j)+b_{mn}^j\mathbf{n}_{mn}^{(3)}(j)) \quad (3)$$

where $a_{mn}^j=-p_{mn}^j\beta_n^{j,(L+1)}$ and $b_{mn}^j=-q_{mn}^j\alpha_n^{j,(L+1)}$ are the scattering coefficients, p_{mn}^j, q_{mn}^j are the coefficients for the applied incident plane wave, and $\alpha_n^{j,(L+1)}$ and $\beta_n^{j,(L+1)}$ are scattering wave coefficients for the jth nanoshell .

By the vector addition theorem, the scattered field of the ith particle written for its coordinates is translated into the

ISBN: 978-988-19252-9-9
ISSN: 2078-0958 (Print); ISSN: 2078-0966 (Online)

incident field for the *j*th particle with the coordinates fixed at the *j*th particle by the following transformations,

$$\mathbf{m}_{mn}^{(3)}(i)=\sum_{\mu=1}^{\infty}\sum_{\nu=-\mu}^{\mu}\left(A_{mn}^{\mu\nu}(i,j)\mathbf{m}_{\mu\nu}^{(1)}(j)+B_{mn}^{\mu\nu}(i,j)\mathbf{n}_{\mu\nu}^{(1)}(j)\right)$$
$$\mathbf{n}_{mn}^{(3)}(i)=\sum_{\mu=1}^{\infty}\sum_{\nu=-\mu}^{\mu}\left(B_{mn}^{\mu\nu}(i,j)\mathbf{m}_{\mu\nu}^{(1)}(j)+A_{mn}^{\mu\nu}(i,j)\mathbf{n}_{\mu\nu}^{(1)}(j)\right) \quad (4)$$

where (*i*) means that the wave functions **m** and **n** are written in the coordinates fixed at the *i*th nanoshell, and the coefficients for the transformation are $A_{mn}^{\mu\nu}(i,j)$ and $B_{mn}^{\mu\nu}(i,j)$ given in [8]. After the transformation has been applied to all nanoshells in the aggregate, the boundary conditions at the outer surface of the *j*th nanoshell yield the expressions for the coefficients of the scattered field of the *j*th nanoshell as related to the same coefficients of other nanoshells. This procedure results in a system of equations with the scattered field coefficients for each nanoshell being the unknowns, which can be solved by matrix inversion.

The absorption cross section for the *i*th particle in the aggregate can be calculated by the following expression,

$$C_{abs}^{i}=\frac{4\pi}{k^2\,|\,m_l^i\,|^2}\mathrm{Re}\sum_{n=1}^{\infty}\sum_{m=-1}^{m=1}i\frac{n(n+1)}{2n+1}\frac{(n+m)!}{(n-m)!}\left(C_1^i+C_2^i+C_3^i\right) \quad (5)$$

where

$$C_1^i=\psi_n\,'(m_L^i x_L^i)\psi_n^*(m^i x_L^i)(m^i c_{mn}^{i,(L)}c_{mn}^{*i,(L)}+m^{*i}d_{mn}^{i,(L)}d_{mn}^{*i,(L)})$$
$$C_2^i=\xi_n\,'(m_L^i x_L^i)\xi_n^*(m_L^i x_L^i)(m^i b_{mn}^{i,(L)}b_{mn}^{*i,(L)}+m^{*i}a_{mn}^{i,(L)}a_{mn}^{*i,(L)})$$
$$C_3^i=\sum_{l=1}^{\infty}\begin{Bmatrix}\mathrm{Re}[i\psi_n^*(m_L^i x_L^i)\xi_n'(m_L^i x_L^i)(mc_{mn}^{*i,L}b_{mn}^{i,L}+m^*d_{mn}^{*i,L}a_{mn}^{i,L})]+\\ \mathrm{Re}[i\psi_n\,'(m_L^i x_L^i)\xi_n^*(m_L^i x_L^i)(mc_{mn}^{i,L}b_{lmn}^{*i,L}+m^*d_{mn}^{i,L}a_{mn}^{*i,L})]\end{Bmatrix} \quad (6)$$

and coefficients c_{mn} and d_{mn} and be calculated in[9].

The total absorption cross section is given by $C_{abs}=\sum_l^L C_{abs}^l$. The internal field can now calculated using Eqs. (2) and (3). Knowing the internal field, one can determine the heat generation in a metal layer, which is the real part of the divergence of the Poynting vector.

The internal field can be calculated using Eqs. (2) and (3), once the coefficients are known. Knowing the internal field, one can calculate the heat generation in a metal layer, which is the real part of the divergence of the Poynting vector ,

$$p=\mathrm{Re}[-\nabla\cdot\mathbf{S}^*]=\frac{1}{2}\sigma\mathbf{E}\square\mathbf{E}^* \quad (7)$$

where $\sigma=\mathrm{Re}[i\omega\varepsilon^*]$, $\varepsilon=m^2$ and the time-averaged Poyting vector S^* is defined as

$$\mathbf{S}^*=\frac{1}{2}\mathbf{E}\times\mathbf{H}^*=i\omega\left(\frac{\mu}{2}\mathbf{H}\cdot\mathbf{H}^*-\frac{\varepsilon}{2}\mathbf{E}\cdot\mathbf{E}^*\right) \quad (8)$$

with * denoting the complex conjugate.

B. Solution of Energy Balance Equation

Knowing the heat flow rate $g(r,\theta,\phi,t)$ of a nanoparticle, the temperature field of such a particle embedded in an infinite media, e.g. bio-tissue, can be described by energy balance equation in spherical coordinate,

$$\frac{1}{r^2}\frac{\partial}{\partial r}\left(r^2\frac{\partial T}{\partial r}\right)+\frac{1}{r^2\sin\theta}\frac{\partial}{\partial\theta}\left(\sin\theta\frac{\partial T}{\partial\theta}\right)+\frac{1}{r^2\sin^2\theta}\frac{\partial^2 T}{\partial\phi^2}+\frac{g(r,\theta,\phi,t)}{K}=\frac{1}{\alpha}\frac{\partial T}{\partial t} \quad (9)$$

with the boundary and initial conditions,

$$\begin{cases}T_1=Finite & r=0\\ T_1=T_2 & r=a\\ -K_1\dfrac{\partial T_1}{\partial r}=-K_2\dfrac{\partial T_2}{\partial r} & r=a\\ T_2=T_3 & r=b\\ -K_2\dfrac{\partial T_2}{\partial r}=-K_3\dfrac{\partial T_3}{\partial r} & r=b\\ T_2=T_\infty & r\to\infty\\ T=T_\infty & t=0\end{cases} \quad (10)$$

The above equations can be solved using the Laplace transform, Green's function or integral transform method [9]. Unfortunately, the first two of them cannot be directly used here without a considerable mathematical effort. For a multiple domain problem, it can be rather difficult to obtain an inverse expression for the Laplace transform or to construct an appropriate Green's function. The integral transform method is relatively easier among the three, and yet its use for the solution of heat conduction equation in infinite domains in spherical coordinates has not been attempted. Here starting with the eigen functions, we present a systematic approach to construct the direct and inverse integral transform needed for a non-homogeneous heat conduction problem defined over a multiple domain with an infinite boundary.

A nanoshell in a finite host medium

To facilitate the derivation, new variables $\mu=\cos\theta$ and $V(r,\theta,\phi,t)=r^{1/2}\left(T(r,\theta,\phi,t)-T_\infty\right)$ are introduced, and Eq. (9) is re-written as

$$\frac{1}{r}\frac{\partial}{\partial r}\left(r\frac{\partial V}{\partial r}\right)-\frac{V}{4r^2}+\frac{1}{r^2}\frac{\partial}{\partial\mu}\left((1-\mu^2)\frac{\partial V}{\partial\mu}\right)+\frac{1}{r^2(1-\mu^2)}\frac{\partial^2 V}{\partial\phi^2}+\frac{g^*(r,\theta,\phi,t)}{K}=\frac{1}{\alpha}\frac{\partial V}{\partial t} \quad (11)$$

where $g^*(r,\mu,\phi,t)=g(r,\mu,\phi,t)\sqrt{r}$.

The eigen function for the inner silica core, gold shell, and finite host media are

$$R_1(r,\beta)=J_{n+1/2}(\frac{\beta}{\sqrt{\alpha_1}}r) \quad (12)$$

$$R_2(r,\beta)=A(\beta)J_{n+1/2}(\frac{\beta}{\sqrt{\alpha_2}}r)+B(\beta)J_{-n-1/2}(\frac{\beta}{\sqrt{\alpha_2}}r) \quad (13)$$

$$R_3(r,\beta)=C(\beta)J_{n+1/2}(\frac{\beta_3}{\sqrt{\alpha_3}}r)+D(\beta)J_{-n-1/2}(\frac{\beta_3}{\sqrt{\alpha_3}}r) \quad (14)$$

The constants $A(\beta)$、$B(\beta)$、$C(\beta)$、$D(\beta)$ can be determined by applying the boundary conditions, with the results,

$$A=-\frac{\pi a}{2}\left(\frac{J_{n+1/2}(\lambda_1 a)J'_{-n-1/2}(\lambda_2 a)-KJ_{-n-1/2}(\lambda_2 a)J'_{n+1/2}(\lambda_1 a)-J_{n+1/2}(\lambda_1 a)J_{-n-1/2}(\lambda_2 a)(1-K)}{2a}\right)$$

$$B=-\frac{\pi a}{2}\left(\frac{KJ_{n+1/2}(\lambda_2 a)J'_{n+1/2}(\lambda_1 a)-J_{n+1/2}(\lambda_1 a)J'_{n+1/2}(\lambda_2 a)+(1-K)J_{n+1/2}(\lambda_2 a)J_{n+1/2}(\lambda_1 a)}{2a}\right)$$

$$C=-\frac{\pi b}{2}\begin{bmatrix}R_2J'_{-n-1/2}(\lambda_3 b)-R_2J_{-n-1/2}(\lambda_3 b)(1-K_{23})/2b\\ -K_{23}R_2\,'J_{-n-1/2}(\lambda_3 b)\end{bmatrix}$$

ISBN: 978-988-19252-9-9
ISSN: 2078-0958 (Print); ISSN: 2078-0966 (Online)

$$D=-\frac{\pi b}{2}\begin{bmatrix}K_{23}J_{n+1/2}(\lambda_3 b)R_2'+R_2(1-K_{23})J_{n+1/2}(\lambda_3 b)/2b\\-R_2J'_{n+1/2}(\lambda_3 b)\end{bmatrix}$$

It is straightforward to show that the eigen functions satisfy the following orthogonal condition,

$$\sum_{i=1}^{M}\frac{k_i}{\alpha_i}\int_{l_i} rR_i(\beta_n,r)\cdot R_i(\beta_m,r)dr=\begin{cases}0 & n\neq m\\ N(\beta_n) & n=m\end{cases} \quad (15)$$

where α_i and K_i ($i=1,2,...M$) denote the thermal diffusivity and conductivity, respectively, with M being the number of the materials or domains. For the present problem, M=3, and i=1, stands for the SiO_2 core, i=2for the gold nanoshell, and i=3 for the surrounding tumor. With L taken as the radius of the tumor region, $N(\beta_n)$ can be obtained as follows,

$$N(\beta_n)=\sum_{i=1}^{M}\frac{k_i}{\alpha_i}\int_{l_i} rR_i^2(\beta_n,r)dr$$
$$=\frac{K_1}{\alpha_1}\int_0^a rR_1^2(\beta_n,r)dr+\frac{K_2}{\alpha_2}\int_a^b rR_2^2(\beta_n,r)dr+\frac{K_3}{\alpha_3}\int_b^L rR_3^2(\beta_n,r)dr \quad (16)$$

A series of direct and inverse transforms leads to the following expressions,

$$\tilde{\bar{V}}_i(r,n,m,t)=\sum_{v=1}^{\infty}\frac{R_i(\beta_v,r)}{N(\beta_v)}\tilde{\hat{V}}(\beta_v,n,m,t)$$
$$\bar{V}(r,\mu,m,t)=\sum_{m=0}^{n}\sum_{v=1}^{\infty}\frac{P_m^n(\mu)}{G(m,n)}\frac{R_i(\beta_v,r)}{N(\beta_v)}\tilde{\hat{V}}(\beta_v,n,m,t)$$
$$V_i(r,\mu,\phi,t)=\sum_{n=0}^{\infty}\sum_{m=0}^{n}\sum_{v=1}^{\infty}\frac{1}{f(m)}\frac{P_m^n(\mu)}{G(m,n)}\frac{R_i(\beta_v,r)}{N(\beta_v)}\tilde{\hat{V}}(\beta_v,n,m,t) \quad (17)$$

whence the transient temperature in the medium where the nanoshell is embedded can be obtained,

$$T_i(r,t)-T_\infty=r^{-1/2}V_i(r,\mu,\phi,t) \quad (18)$$

A nanoshell in an infinite host medium

If the surrounding medium, e.g. tumor tissue, extends to infinity, there exist two problems for the above solution: (1) $N(\beta_n)\to\infty$ and (2) β is no longer discrete in value. Following the normal procedure, one can show that

$$\frac{K_3}{\alpha_3}\int_b^{L\to\infty} rR_3^2(\beta_n,r)dr$$
$$=\frac{K_3}{\alpha_3}\int_b^{L\to\infty} r\left(C(\beta)J_{n+1/2}(\frac{\beta_3}{\sqrt{\alpha_3}}r)+D(\beta)J_{-n-1/2}(\frac{\beta_3}{\sqrt{\alpha_3}}r)\right)^2 dr$$
$$=\frac{K_3}{\alpha_3}\int_b^{L\to\infty} r\begin{pmatrix}C^2J_{n+1/2}^2(\lambda r)+D^2J_{-n-1/2}^2(\lambda r)\\+2CDJ_{n+1/2}(\lambda r)J_{-n-1/2}(\lambda r)\end{pmatrix}dr \quad (19)$$

where $\lambda=\beta/\sqrt{\alpha_3}$.

Making use of the asymptotic expression for the Bessel function,

$$J_v(\lambda r)\cong\sqrt{\frac{2}{\pi\lambda r}}\cos\left(\lambda r-\frac{\pi}{4}-\frac{v\pi}{2}\right) \quad (20)$$

One can show that the first and second terms in Eq. (16) are finite and that the third term becomes $K_3(\alpha_3)^{-1}\int_b^{L\to\infty} rR_3^2(\beta_n,r)dr\to\infty$.

For a meaningful solution, $N(\beta_n)$ must be finite. To overcome this difficulty, we thus re-define the normalization factor by introducing a factor, $c_N=\beta\pi\sqrt{\alpha_3}/L$ and thus we have

$$\hat{N}(\beta_n)=\lim_{L\to\infty}\frac{\beta\pi\sqrt{\alpha_3}}{L}\hat{N}(\beta_n)=\lim_{L\to\infty}\frac{\beta\pi\sqrt{\alpha_3}}{L}\frac{K_3}{\alpha_3}\frac{L\sqrt{\alpha_3}}{\pi\beta}\left(C^2+D^2\right) \quad (21)$$

With a re-defined norm, the inverse transform can be re-written in an integral form,

$$\tilde{\bar{V}}_i(r,n,m,t)=\sum_{\substack{v=1\\ \beta\to 0}}^{\infty}\frac{R_i(\beta_v,r)}{N(\beta_v)}\tilde{\hat{V}}(\beta_v,n,m,t)$$
$$=\sum_{\substack{v=1\\ \beta\to 0}}^{\infty}\frac{R_i(\beta_v,r)}{N(\beta_v)c_N}\tilde{\hat{V}}(\beta_v,n,m,t)\beta\Delta\beta \quad (22)$$
$$=\int_0^{\infty}\frac{R_i(\beta,r)}{\hat{N}(\beta)}\tilde{\hat{V}}(\beta,n,m,t)\beta d\beta$$

$$\bar{V}_i(r,\mu,m,t)=\sum_{m=0}^{n}\int_0^{\infty}\frac{P_n^m(\mu)}{G(m,n)}\frac{R_i(\beta,r)}{\hat{N}(\beta)}\tilde{\hat{V}}(\beta,n,m,t)\beta d\beta$$

$$V_i(r,\mu,\phi,t)=\sum_{n=0}^{\infty}\sum_{m=0}^{n}\int_0^{\infty}\frac{1}{f(m)}\frac{P_n^m(\mu)}{G(m,n)}\frac{R_i(\beta,r)}{\hat{N}(\beta)}\tilde{\hat{V}}(\beta,n,m,t)\beta d\beta$$

from which the final expression for the temperature distribution is obtained

$$T_i(r,\mu,\phi,t)-T_\infty=r^{-1/2}V_i(r,\mu,\phi,t)$$
$$=\frac{1}{r^{1/2}K_3}\sum_{n=0}^{\infty}\sum_{m=0}^{n}\frac{1}{f(m)}\frac{P_n^m(\mu)}{G(m,n)}\int_0^{\infty}\frac{1-e^{-\beta^2 t}}{\beta}\frac{R_i(\beta,r)}{C(\beta)^2+D(\beta)^2}$$
$$\int_a^b r'^{3/2}R_2(\beta,r')\tilde{\bar{g}}_2^{\,*}(r',n,m,t)dr'd\beta \quad (23)$$

III. Results and Discussion

A. *Joule Heat Distribution in a nanoshell*

Besides the overall absorption and scattering behavior of nanoshells, detailed heat generation and its distribution inside the conductive metal shell is also of importance to assess the local thermal environment. Figure 1 illustrates the absorbed power generation in and the energy distribution around an individual gold nanoshell of 72nm:60nm in size. The nanoshell is surrounded by water and illuminated by an *x*-polarized *z*-direction propagating plane wave. Figure 1(a) depicts the normalized energy distribution in the *XOY* cross section under resonance condition. Apparently, the strongest SPR-induced field enhancement occurs near the outer surface. Figure 1(b) shows the distribution of Joule heat in metal layer, which reveals that near the regions where the field enhancement is strongest, the heat generation inside the gold shell is the lowest. For example, in Fig. 1(a) the maximal field enhancement occurs at the two ends along x-axis, i.e. along the polarization direction. However, in the gold shell, the heat generation at these two ends attains a minimum. This can be explained by the fact that the applied external field is reversely superimposed with the polarization field inside the nanoshell, while outside the nanoshell, it is just the opposite. Figure 1(c) gives a three dimensional view of the distribution of Joule heat on the outermost spherical surface at dipole SPR

ISBN: 978-988-19252-9-9
ISSN: 2078-0958 (Print); ISSN: 2078-0966 (Online)

mode. Clearly, the absorbed energy unevenly spreads in the metal layer with strong heating taking place around the equator.

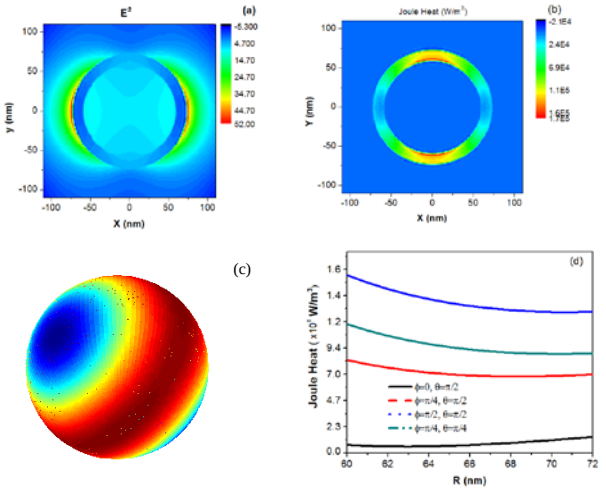

Fig. 1 The field enhancement and loss distribution in a gold nanoshell: (a) Energy contour in *XOY* plane at 795nm (b) Distribution of Joule heat within the gold shell, (c) 3-D distribution of Joule heat on the outer surface of gold shell, and (d) Joule heat along radial direction.

The detailed radial distribution of absorbed energy is plotted in Fig. 1(d). It can be seen that the energy absorbed near the core-shell interface is even higher than that at the outer shell surface, in contrast with the well-known electromagnetic skin depth decay. This phenomenon is apparently a result of interaction between the electromagnetic wave and a nano-cavity. Light penetrating through the nano-sized shell into the cavity is confined within and undergoes repeated reflections by the cavity wall until they are absorbed by the metal, thereby giving rise to the non-classical profile.

B. Energy absorbed by aggregated nanoparticles

The modeling study is now extended to investigate the absorption by a nanoshell cluster or a group of clusters. Our laboratory experiments show that nanoshells, when made in solution, tend to cluster together due to the imbalance of electrostatic and the *van der Waals* force between particles. Model simulations were conducted for various scenarios and selected results are given in Fig. 2. The particles in the cluster are the same, all with 60nm-radius silica core, a 12nm-thick gold shell, and with three particles along each axial direction. The interpartice surface-to-surface distance (designated by *g*) is kept as a vaiable. The averaged absorption efficiency (total absorption efficiency divided by the total number of nanoparticle number, NT=7 in this case) is used. From Fig. 2(a), it is clear that both the resonance wavelength and the averaged absorption efficiency are different from the counterparts of an isolated nanoshell. This change in the total absorption is caused by the combined coupling effect as discussed in the previous section, that is, the electromagnetic coupling of nanoshells along the polarization direction results in a dominant red-shift in the collective resonance of a particle aggregate, while the interaction between particles perpendicular to polarization direction causes the resonance peak to shift only slightly. The magnitude of the absorption efficiency depends on the interparticle spacing, however.

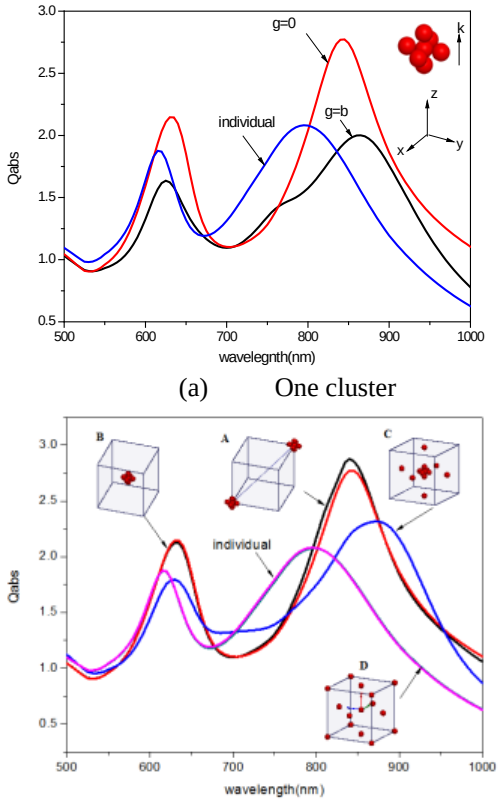

(a) One cluster

(b) Two clusters

Fig.2 Absorption spectrum of aggregated nanoshells

The energy absorption by an assemble of 13~15 nanshells is calculated and given in Fig. 2(b) for different spatial arrangement within the same space volume. Curve A considers two clusters. The center-to-center spacing of the two clusters is 20b=1440nm. The average Qabs is compared with that of a single cluster (curve B) and of an isolated nanoshell. Since the spacing of the two clusters is greater than one wavelength, the interaction between the clusters is insignificant. This is the reason why curve A is almost the same as curve B. Both curves, however, are different from that of an isolated nanoshell. In Case C, a center cluster is surrounded by the rest of the nanoshells uniformly dispersed. Finally, curve D is the case where one particle is at the center of the cube, and the other fourteen nanoshells spread at the vertex or the face center of the cube. It is found that the average absorption spectrum of group D almost coincides with that of individual nanoshell. This is attributed to the weak coupling effect due to large interparticle separations.
The results in Fig. 2 suggest that the aggregation of nanoshells can have a strong effect on the plasmonic absorption. Both absorption magnitude and resonance wavelength can differ from that of an individual particle considerably. This effect should be accounted for when specific thermal applications involving nanoshells are considered.

C. Temperature profile in an isolated nanoshell

Assume an isolated gold nanoshell with size of 60/72nm embedding in a tumor. Compared to the nanoparticle, tumor is basically in mm-scale size, and thus can be regarded as an infinite host media in size. A laser with intensity of $0.0017W/m^2$ (equivalent to $E_0 = 1V/m$) and 800nm wavelength is employed to induce the plasmonic heating inside the nanoshell.

ISBN: 978-988-19252-9-9
ISSN: 2078-0958 (Print); ISSN: 2078-0966 (Online)

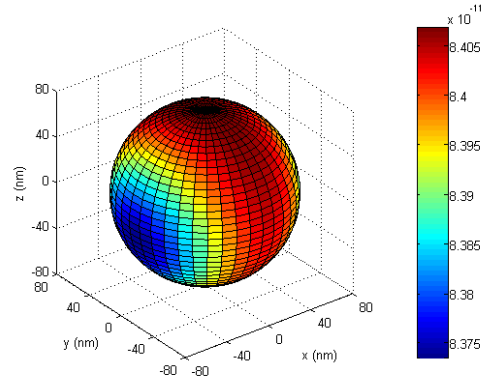

(a) temperature distribution on the outer shell surface

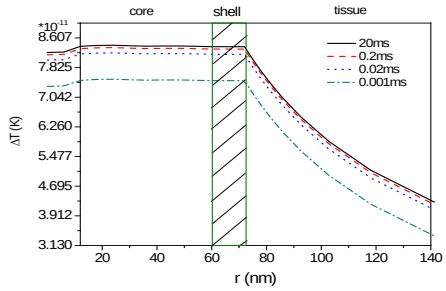

(b) temperature distribution in an Au nanoshell system

Fig. 3 Temperature field in and around an isolated nanoparticle.

Figure 3 illustrates the temperature profile in and around the SiO_2-gold core-shell nanostructure embedded in a tissue medium at *t=20ms*. Fig. 3a shows the temperature distribution on the outer surface of the gold layer, which is in agreement with the Joule heat distribution shown in Fig. 1. The highest temperature rise is $T_{\max} = 8.403\times10^{-11}$ K. Here the temperature means the temperature departure from T_∞. In the direction parallel to the electric field, temperature is the lowest. Further investigation shows that the maximum temperature difference within the particle along the radial direction and circumferential direction are 0.02% and 0.22%, respectively. It thus can be concluded that the heating in a nanoshell is rather uniform.

It should be stated that the size effect and time effect on thermo physical properties of metal in nanoscale were not taken into account in the above analysis. The present work presents a mathematical framework for integrated mathematical photo-thermal analysis. If needed, the effect of thermal transport in nanoscale may be realized by modifying the thermal parameters.

D. Simplified heat conduction model of a tumor with nanoshells

The above discussion provides a direct and efficient way to analayze the heat transfer phenomena in and outside of a concentric nanoparticle. In most real applications, especially in thermal therapy, use is made of nanoparticles in a huge number. It is impractical to simulate each of nanoparticles in the system, although the mathematical model presented in this paper can be used in theory for this purpose. Here a simplified heat conduction model may be considered for biotissue thermal analysis.

Nanoshells are often conjugated with a cancer targeting agent and passively accumulated in tumor by intravenous injection. With a reasonable low dose of nanoshells for a therapeutic treatment, the inter-particle electromagnetic coupling may be neglected as a first approximation. Our calculations show that with the inter-particle space bigger that 20 times particle diameter, the nanoparticle can be regarded as optically isolated. This implies that the absorption of each particle is approximately the same and is independent of each other.

Based on the above consideration, a simplified heat conduction model of tumor with nanoshells can be developed. The tumor embedded with nanoshells is an equivalent heat generator, surrounded by infinite host media, i.e. healthy tissue. Thus, Eq. (23) becomes one dimensional,

$$\Delta T_i(r,t) = \frac{Q_c}{r^{1/2}K_2}\int_0^\infty \frac{1-e^{-\beta^2 t}}{\beta}\frac{R_i(\beta,r)\int_a^b r'^{3/2}R_1(\beta,r')dr'}{A(\beta)^2+B(\beta)^2}d\beta \tag{24}$$

The steady-state temperature in tumor is given by

$$\Delta T_1(r) = Q_c\left(-\frac{r^2}{6K_1}+\frac{r_t^2}{6K_1}+\frac{r_t^2}{3K_2}\right) \tag{25}$$

and that in the healthy tissue by

$$\Delta T_2(r) = \frac{Q_c r_t^3}{3rK_2} \tag{26}$$

To evaluate the equivalent model qualitatively, computations were carried out with the parameters taken according to the experiment given in literature [10].

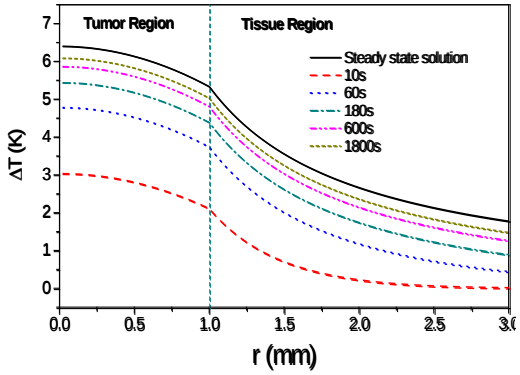

Fig.4 Temperature rise in tumor and healthy tissues, where f_m = 12.5 *ppm* and the vertical axis stands for temperature departure from T_∞. The parameters used for calculations: size of nanoshell=71.5/59.5nm, mass concentration=12.5ppm, intensity of laser=4W/cm^2, wavelength of laser=808nm, spot diameter of laser=5mm, duration of thermal treatment = 3min, and tumor size (diameter) = 2 mm.

At a 12.55ppm, the inter-particle space among nanoshells is 73 times diameter if the nanoshells are assumed to be distributed uniformly. This would satisfy the condition of optical isolation. The temperature (relative to a standard temperature) increase inside and outside the tumor at different times are shown in Fig.4. At *t*=3min, the temperature goes up to 5.44K. Taking T_∞=37 ^{o}C as a normal body temperature for comparison, temperature inside the tumor reaches to 42.44 ^{o}C, which just meets the equipment of hyperthermia treatment. With time elapse, the temperature keeps increasing until the steady state is reached: 6.4K inside the tumor. Although the exact temperature was not provided in Ref. [10], all the data

ISBN: 978-988-19252-9-9
ISSN: 2078-0958 (Print); ISSN: 2078-0966 (Online)

from the analysis appear to be in a reasonable range. This implies the feasibility of the equivalent model.

IV. Conclusion

A modeling study of energy absorption and heat conduction in concentric nanoparticles has been presented. Results show that the radial distribution of the absorbed power in metal layer may differ from the classical skin depth phenomena due to the presence of dielectric cavity inside the shell. The energy absorbed by aggregates depends on the inter-particle spacing. Proximity effect causes the energy absorption of clusters to differ considerably from that of an isolated particle. For a low concentration dose in thermal treatment, nanoparticles may be taken to be optically isolated. Analytical solution for a cluster of optically isolated nanoshells and simplified model for a tumor with huge number of nanoshells were presented and verified qualitatively.

Acknowledgment

We gratefully acknowledge the financial support of Shanghai Natural Science Foundation (No. 11ZR1417300), and Medical-Engineering Joint Funds of Shanghai Jiao Tong University (No. YG2011MS25).

References

[1] J. H. Lee, Q. Wu, and W. Park, *J. Mater. Res.* 21, 3215 (2006).
[2] N. Garrett, M. Whiteman, and Julian Moger, *Optics Express*, 19, 17563 (2011).
[3] C. Loo, L. Hirsch, and M.H. Lee, *Optical Letters*, 30, 1012 (2005).
[4] L. B. Carpin, L. R. Bickford, G. Agollah, T. K. Yu, R. Schiff, Y. Li, and R. A, Drezek, *Breast Cancer Research and Treatment*, 125, 27 (2011).
[5] J. B. Lassiter, J. Aizpurua, L. I. Hernandez, D. W. Brandl, I, Romero, S. Lal, J. H. Hafner, P. Nordlander, and N. J. Halas, *Nano Lett.* 8, 1212 (2008).
[6] Bohren CF and Huffman DR, *Absorption and scattering of light by small particles*, New York: Wiley (1983).
[7] C. Liu and B. Q. Li, J. Phys. Chem. C, *115, 5323 (2011).*
[8] A. Messiah A, *Quantum mechanics*, Dover, New York (1981).
[9] M. Necati Ozisik, *Heat Conduction*, Wiley, New York, (1980)
[10] Gobin AM, Lee MH, Halas NJ, et al., *Nano Lett.* 7:1929(2007)

ISBN: 978-988-19252-9-9
ISSN: 2078-0958 (Print); ISSN: 2078-0966 (Online)